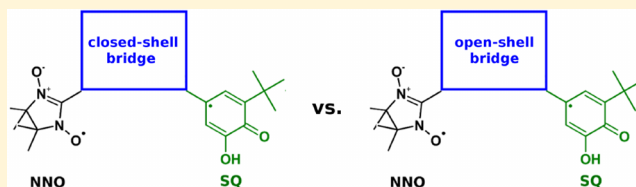


Influence of Radical Bridges on Electron Spin Coupling

Torben Steenbock,[†] David A. Shultz,[‡] Martin L. Kirk,[¶] and Carmen Herrmann^{*,†}[†]Institute of Inorganic and Applied Chemistry, University of Hamburg, Martin-Luther-King-Platz 6, 20146 Hamburg, Germany[‡]Department of Chemistry, North Carolina State University, Raleigh, North Carolina 27695-8204, United States[¶]Department of Chemistry and Chemical Biology, University of New Mexico, Albuquerque, New Mexico 87131-0001, United States

Supporting Information

ABSTRACT: Increasing interactions between spin centers in molecules and molecular materials is a desirable goal for applications such as single-molecule magnets for information storage or magnetic metal–organic frameworks for adsorptive separation and targeted drug delivery and release. To maximize these interactions, introducing unpaired spins on bridging ligands is a concept used in several areas where such interactions are otherwise quite weak, in particular, lanthanide-based molecular magnets and magnetic metal–organic frameworks. Here, we use Kohn–Sham density functional theory to study how much the ground spin state is stabilized relative to other low-lying spin states by creating an additional spin center on the bridge for a series of simple model compounds. The di- and triradical structures consist of nitronyl nitroxide (NNO) and semiquinone (SQ) radicals attached to a *meta*-phenylene(R) bridge (where R = $-\text{NH}^\bullet/-\text{NH}_2$, $-\text{O}^\bullet/\text{OH}$, $-\text{CH}_2^\bullet/\text{CH}_2$). These model compounds are based on a fully characterized SQ–*meta*-phenylene–NNO diradical with moderately strong antiferromagnetic coupling. Replacing closed-shell substituents CH_3 and NH_2 with their radical counterparts CH_2^\bullet and NH^\bullet leads to an increase in stabilization of the ground state with respect to other low-lying spin states by a factor of 3–6, depending on the exchange–correlation functional. For OH compared with O^\bullet substituents, no conclusions can be drawn as the spin state energetics depend strongly on the functional. This could provide a basis for constructing sensitive test systems for benchmarking theoretical methods for spin state energy splittings. Reassuringly, the stabilization found for a potentially synthesizable complex (up to a factor of 3.5) is in line with the simple model systems (where a stabilization of up to a factor of 6.2 was found). Absolute spin state energy splittings are considerably smaller for the potentially stable system than those for the model complexes, which points to a dependence on the spin delocalization from the radical substituent on the bridge.



1. INTRODUCTION

Controlling the relative orientation of local electron spins in the ground state is an important goal in molecular magnetism¹ and molecular spintronics.² This relative orientation is often dominated by exchange coupling and/or spin polarization,³ which leads to either ferromagnetic (parallel) or antiferromagnetic (antiparallel) alignment of the spins in the ground state and which can be mediated over quite long distances via closed-shell subunits (superexchange).^{1,3–6} In addition to the local spin arrangement in the ground state, the energetic separation from other relative spin orientations is important for designing molecule-based magnets and spintronic devices or materials.

For certain lanthanide complexes, it has been found that while they exhibit remarkable single-ion magnetic anisotropy, coupling of multiple magnetic centers by typical closed-shell bridging ligands is weak. Long and co-workers solved this problem by introducing a spin-polarized bridge^{7–10} that couples antiferromagnetically to each lanthanide center, resulting in parallel alignment of the (larger) lanthanide magnetic moments and a considerably larger total magnetic moment. Related complexes have been synthesized and characterized using organic radical bridging ligands^{11–13} and 3d transition-metal centers.¹⁴

Radical bridges are also interesting for other cases in which closed-shell linkers only weakly couple spins, such as magnetic metal–organic frameworks (MOFs),^{15,16} where spin-polarized transition-metal centers are bridged by organic linkers. The length of these organic linkers is known to play a decisive role in tuning the pore size.^{17,18} With increasing length of the linkers, the interactions between the spin centers decrease (often but not necessarily exponentially^{3–6}). This problem may be solved by employing radical linkers, which could mediate the exchange spin coupling between the magnetic subunits and stabilize the ground state against the remaining spin states.¹⁹ A first example of a porous material based on a covalent organic framework of nickel porphyrins with postsynthetically functionalized radical linkers was given in 2015, but the focus was on electrochemical energy storage and not on magnetic properties.²⁰ Otherwise, several MOFs with radical linkers have been synthesized, but so far, a combination of magnetic properties with suitable permanent porosity has been difficult to realize.

Received: July 20, 2016

Revised: December 6, 2016

Published: December 6, 2016



Radical bridging ligands have also been studied with respect to their influence on the electronic structure of ruthenium mixed-valence complexes^{21,22} and on the charge-recombination dynamics in electron donor–bridge–electron acceptor systems, for which the effects of introducing different spin densities on the bridge have been studied using *tert*-butylphenylnitroxide radical groups centrally attached to meta-linked phenyl bridges.^{23,24} Spin-bearing mixed-valence semiquinone (SQ)–Co(III)(pyridine)₂–catecholates linking nitronyl nitroxide (NNO) radicals have also been investigated as model systems for exchange interactions between localized spins and the spins of itinerant electrons.²⁵

While the idea of using radical linkers or bridges for increasing interactions between spin centers has been widely accepted and applied, there exists a dearth of systematic studies on the relation between the chemical structure of the radical bridge and (a) the spin arrangement in the ground state and (b) its stabilization with respect to spin excitations. Our goal is to assess by how much spin-polarized bridging ligands can stabilize the relative local spin orientation in the ground spin state, measured as the energy between the ground state and the first excited spin state (obtained by inverting the spin orientation on one spin center), using Kohn–Sham density functional theory (KS-DFT) calculations. Because spin state energetics are known to depend strongly on the approximate exchange–correlation functional, in particular, on the amount of exact exchange admixture,^{26,27} we compare a range of functionals with different amounts of exact exchange, including the double-hybrid B2PLYP, in which, apart from replacing part of the exchange functional by a Hartree–Fock expression, a perturbation-theory-based part is mixed into the correlation functional.²⁸ Additionally, we test the influence of Grimme’s empirical dispersion correction.²⁹

As simple computational model systems, we have chosen a set of organic di- and triradicals in which a NNO and a SQ radical with one unpaired electron each are connected by a spin-1/2 *meta*-phenylene(R[•]) bridge (where R[•] = –NH[•], –O[•], –CH₂[•]) or the analogous closed-shell bridges to which the radical units are attached via ethynyl spacers in the meta position relative to NNO and SQ (see Figure 1 for a general

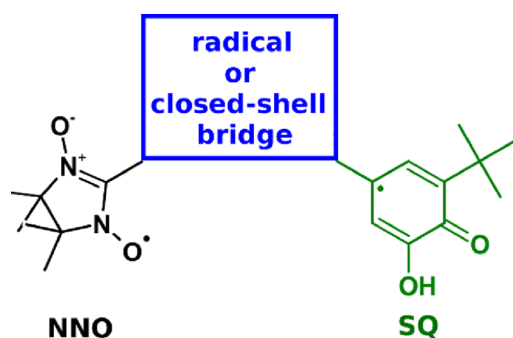


Figure 1. Schematic illustration of the partitioning scheme for the systems under study into the NNO radical, bridge (radical or closed-shell), and SQ radical.

structural model and Figure 2 for detailed structures). In the meta position to these two radicals, a third substituent, X, is attached that may be a radical or a closed-shell group. These structures are abbreviated as NNO–X(Spacer)–SQ. The choice of spin centers was inspired by systems studied experimentally by two of the authors and their co-workers,

modeling the charge-separated state of electron donor–bridge–acceptor systems.⁴ For comparison, para-substituted di- and triradicals were investigated, which due to their asymmetric substitution pattern are synthetically challenging and are therefore discussed in the Supporting Information. The model substituents directly attached to the benzene rings are either small radicals, X=CH₂[•], X=NH[•], and X=O[•], or the corresponding closed-shell groups obtained by adding a hydrogen atom, X=CH₃, X=NH₂, and X=OH. The ethynyl spacers prevent unfavorable steric interactions between the individual components of the system, which ensures that purely electronic effects are studied.

The bridges under investigation here are identical to those studied theoretically in our group with respect to their “spin filtering” properties.³⁰ In that study, significant differences were found between the three radical substituents. As a relationship between electron transport/transfer and exchange spin coupling has been noted since the 1950s,^{4,31–35} it will be interesting to determine whether the three radical substituents also lead to quite different behavior when affecting spin coupling in organic radicals.

The “X” radical substituents are not stable under experimental conditions. Therefore, we additionally consider a complex in which the benzene ring of the bridge is functionalized by a stable nitroxyl radical substituent (abbreviated as NO) or its closed-shell counterpart (NOH), in which the SQ moiety is protected by a zinc complex as employed in previous work⁴ and where the synthetically demanding ethynyl linkers have been eliminated (resulting in the structure NNO–NO–SQ(Zn); see Figure 2). To bridge the gap to the model systems, this structure is compared with NNO–NH–SQ(Zn), NNO–NH–SQ, and the corresponding closed-shell bridge diradicals. Given that these second-generation computational models have been constructed using more chemically stable organic radical substituents on the bridge, they may be regarded as suitable targets for synthetic chemists in the field. This comparison will allow us to judge the transferability of the calculations on model systems to the synthetically accessible ones.

This article is organized as follows: after briefly summarizing the KS-DFT description of organic radicals with multiple spin centers using Noodleman’s broken-symmetry (BS) approach³⁶ and local spin analysis^{37–39} in section 2, we present the computational methodology (section 3). In section 4.1.1, we discuss the dependence of spin state energy splittings on radical versus closed-shell bridges and on the choice of the exchange–correlation functional and then illustrate these findings with plots of magnetic orbitals. In section 4.1.2, we discuss trends in local spin distributions. In section 4.2, the influences of the ethynyl spacer and the stabilizing zinc complex on the spin state energetics and local spins are evaluated, and the potentially synthesizable NNO–NOH/NO–SQ(Zn) di- and triradical pairs are investigated. Additional molecular orbital (MO) plots, local spins for the systems in section 4.2, spin densities, molecular Cartesian coordinates, and results for para-substituted model systems are provided in the Supporting Information.⁴⁰

2. THEORETICAL BACKGROUND

We describe molecular electronic structures and energies in the framework of spin-unrestricted KS-DFT,^{41,42} in which the kinetic energy is calculated using a reference system of noninteracting Fermions and all unknown parts of the

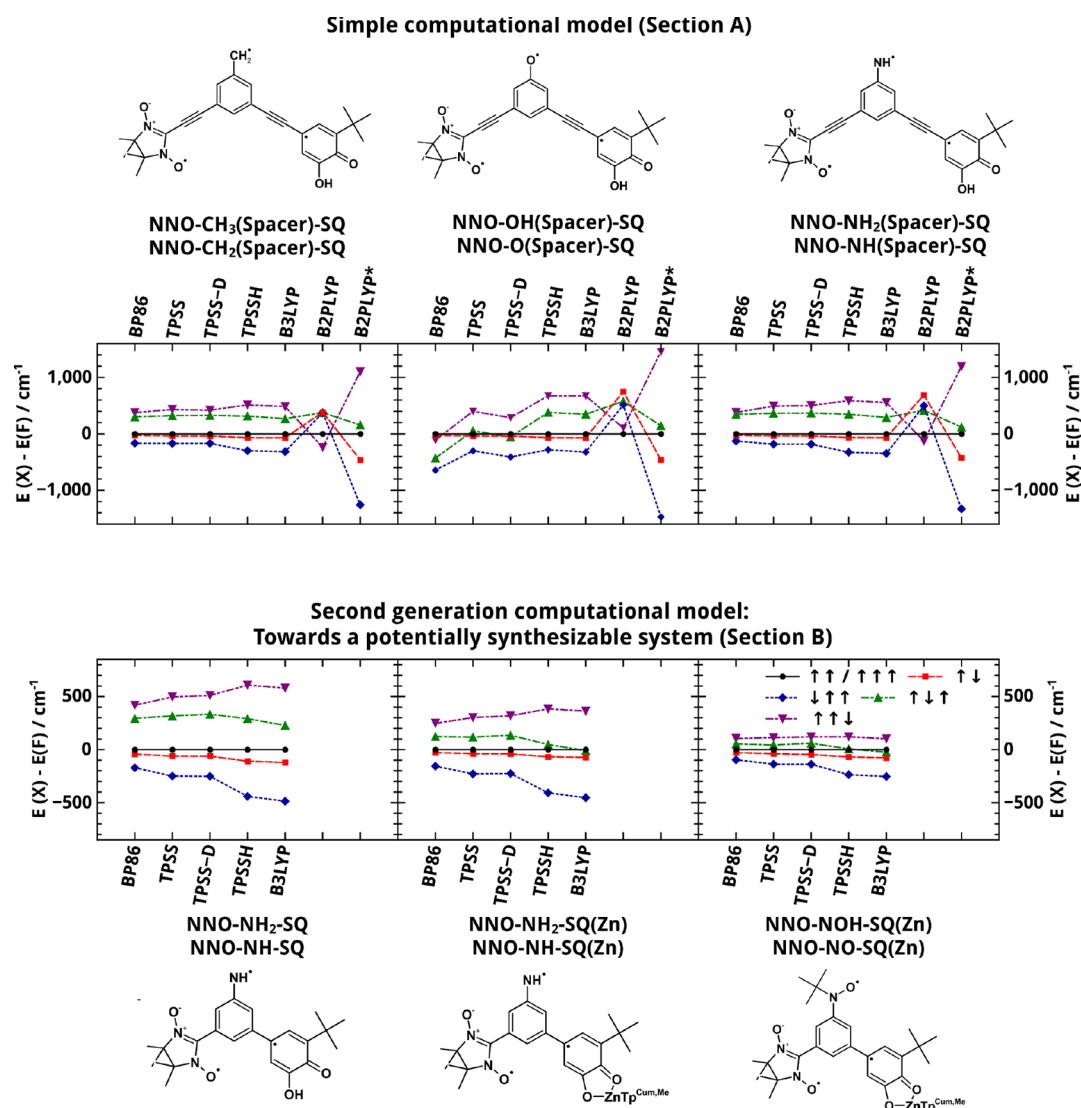


Figure 2. (Top) Relative spin state energies of meta-connected ethynyl-bridged model radicals as studied in section 4.1 for different exchange–correlation functionals (legend given in the bottom right plot). (Bottom) Relative spin state energies of a potential synthetic target NNO–NO–SQ(Zn) system (all three studied in section 4.2). For both diradicals (resulting from a closed-shell bridge) and triradicals (with a radical bridge), energies are given with respect to the ferromagnetically coupled state ($\uparrow\uparrow$ or $\uparrow\uparrow\uparrow$). B2PLYP* refers to the B2PLYP functional employing 100% DFT correlation rather than the original 27% admixture of MP2 correlation.

electronic energy are summarized in an exchange–correlation functional.

The spin multiplicity of a molecule is determined by the expectation value of the total spin operator $\langle\Psi|\hat{S}^2|\Psi\rangle = S(S + 1)\hbar^2$, where S refers to the spin quantum number, \hbar to Planck's constant divided by 2π , and Ψ to the molecular wave function. In the absence of external magnetic fields and neglecting special relativity, the energies of all states of a spin multiplet are the same. While such expectation values are (at least in principle) straightforward to evaluate in wave function theory, it is not clear how to calculate them in KS-DFT. In practice, they are usually obtained by plugging the wave function of the noninteracting Kohn–Sham reference system Φ^{KS} into the expectation value. This practice has been challenged as its theoretical justification is unclear.^{43–51} If one accepts it, the $\langle\Phi^{\text{KS}}|\hat{S}^2|\Phi^{\text{KS}}\rangle$ expectation value can be used as a measure for whether a KS wave function corresponds to a pure spin state, and if it does not, spin projection can be applied to obtain a pure spin state, which for spin states other than the high-spin

state will result in a multireference KS wave function, analogous to wave function theory. Such a procedure based on spin projection has been proposed by Noodleman for calculating Heisenberg coupling constants as a measure of spin coupling from a Kohn–Sham wave function describing a ferromagnetically coupled state (which is usually a pure spin state) and one describing an antiferromagnetically coupled state, which due to its one-determinant nature is usually a mixture of spin states (BS determinant).³⁶ This is the standard approach to spin coupling in quantum chemistry.

It has also been suggested that the spin-symmetry breaking resulting from describing a system with multireference character (in wave function theory) by one determinant in KS-DFT is not only possible but “that the correct solution of the Kohn–Sham equations in LSD or GGA is the fully self-consistent BS single determinant of lowest total energy”⁴³ and that BS DFT yields reliable energies despite its inaccurate spin densities (see ref 51 and references therein). Combinations of KS-DFT with multireference approaches are under steady

development (see, e.g., refs 51 and 52) but not straightforward to employ in practice and computationally far more expensive than KS-DFT.

If one argues that spin projection is not necessary as the obtained $\langle \Phi^{\text{KS}} | \hat{S}^2 | \Phi^{\text{KS}} \rangle$ is not a measure for spin and thus does not prevent the energy of the BS determinant from being interpreted as the energy of the antiferromagnetically coupled state,⁴³ this will result in spin state energies being multiplied by a constant factor (which depends on the number of unpaired spins on each spin center) compared with an approach using spin projection. Because this does not affect qualitative conclusions and because the choice of the exchange–correlation functional typically has a much larger effect on spin state energy splittings than the question of whether to use spin projection or not, for simplicity, we have chosen to directly interpret BS energies as the energies of pure spin states. Their spin multiplicity is evaluated by interpreting the expectation value of the z component of the spin vector, $M_S = \langle \Phi^{\text{KS}} | \hat{S}_z | \Phi^{\text{KS}} \rangle$, as a measure for the spin quantum number S .

Apart from quantitative predictions, a qualitative understanding of magnetic couplings in molecules is essential. An important means of qualitatively characterizing electronic structures is through local properties,⁵³ in this context local spins.^{37–39} These may be obtained by defining atoms (or other subunits) A in molecules in analogy to population analysis, resulting in local spins

$$\langle \hat{S}_{zA} \rangle = \frac{1}{2}(N_A^\alpha - N_A^\beta) \quad (1)$$

where N_A^α is the electron population assigned to center A for spin-up or majority electrons and N_A^β is for spin-down or minority electrons. These may be obtained within the Mulliken partitioning scheme applied here^{54,55} as a sum over matrix product elements for all atom-centered basis functions $|\mu\rangle$ located on A

$$N_A^\alpha = \sum_{\mu \in A} (\mathbf{P}^\alpha \mathbf{S})_{\mu\mu} \quad (2)$$

where \mathbf{P}^α is the density matrix⁵⁵ for spin-up electrons, \mathbf{S} is the basis function overlap matrix with the elements $S_{\mu\nu} = \langle \mu | \nu \rangle$, and N_A^β is defined analogously. It has been shown that while local charges often depend considerably on the atom-centered basis set and on the local partitioning scheme employed, local spins are much more robust with respect to the choice of these parameters.³⁸ A local spin of 1/2 corresponds to one unpaired spin-up electron on this part of the molecular structure.

3. COMPUTATIONAL METHODOLOGY

All molecular structures were optimized within spin-unrestricted KS-DFT for each spin state with the BP86 functional,^{56,57} while for all other functionals, single-point calculations were carried out on the BP86-optimized structures in the respective spin state. Spin state energetics were evaluated with six different exchange–correlation functionals: two pure functionals, BP86^{56,57} and TPSS,⁵⁸ one pure functional featuring Grimme’s dispersion correction, TPSS-D,²⁹ two hybrid functionals with 10 and 20% Hartree–Fock exchange, respectively, TPSSH⁵⁹ and B3LYP,^{60,61} and the double-hybrid functional B2PLYP,²⁸ which features 53% Hartree–Fock exchange and an admixture based on second-order perturbation theory to the correlation functional (results are given in the Supporting Information). Ahlrichs’s triple- ζ split-valence basis

set with polarization functions on all atoms, def-TZVP,^{62,63} was used throughout. For all pure functionals, the resolution-of-the-identity approach was employed.^{64–66} For the self-consistent-field algorithm, a convergence criterion of 10^{-7} au was chosen for the change in energy, and for the molecular structure optimization, a maximum gradient norm of 10^{-4} au was used. The electronic structure calculations in section 4.1 were carried out with TURBOMOLE 6.0, and in section 4.2, they used the TURBOMOLE 6.6 quantum chemistry program packages,^{65,66} respectively.

To obtain electronic structures of BS determinants, a restrained optimization scheme⁶⁷ was used. This term refers to an automatized scheme for guiding the self-consistent field (SCF) algorithm toward a BS solution. In contrast to constrained optimization, where the local spins on the radical centers would be fixed, the algorithm only assures that the values of these local spins are within a window defined by the user. The radical centers for which the local spins are evaluated were defined as the formally spin-carrying atom and all atoms on which this spin is predominantly delocalized, that is, all N and O atoms in the NNO radical and the carbon atom of the SQ ring directly attached to the bridge, along with its two next-nearest neighbors in the ring. This is indicated by the term “restrained”, which is borrowed from Molecular Dynamics simulations. If there is an energetic minimum within this window (which is usually the case if the window is defined by chemically reasonable values), the result is the same as what would have been achieved by an unconstrained optimization but without the need for constructing an elaborate initial guess to ensure convergence to the desired solution.

To evaluate local spins,³⁸ a local version of TURBOMOLE’s MOLOCH was used as implemented at ETH Zurich. MOs were plotted using MOLDEN⁶⁸ and POV-Ray.⁶⁹ All MOs were plotted with an isosurface value of 0.02.

4. RESULTS AND DISCUSSION

The Lewis structures of the triradicals employed in this study (as described in the Introduction) are shown in Figure 2. The orientation of local spins on the NNO, the bridge, and the SQ radical units are designated as “up” (\uparrow) or “down” (\downarrow) (where “up” by convention refers to majority or α spins and “down” to minority or β spins). For example, “ $\uparrow\uparrow\downarrow$ ” refers to a state in which the NNO and the radical substituent on the bridge couple ferromagnetically and the spins on the bridge and on the SQ unit couple antiferromagnetically.

4.1. Model Systems. **4.1.1. Relative Spin State Energies and Frontier Orbitals.** The spin state energies of the diradicals shown in Figure 2 reveal that the meta-connected diradicals with closed-shell bridges have an antiferromagnetically coupled ground state ($\uparrow\downarrow$) for all functionals except for the B2PLYP functional (where we find strong ferromagnetic coupling). Experimental findings for very similar systems suggest that the coupling in the ground state is antiferromagnetic, which is in agreement with our findings (excluding B2PLYP).⁴ The spin state energy splittings obtained from B2PLYP when employing 100% DFT correlation rather than the original 27% admixture of MP2 correlation agree qualitatively (although the quantitative deviations are still large) with the results obtained with other functionals, which indicates that the MP2 part causes these qualitative deviations (see Figure S3 in the Supporting Information).

When using radical bridges for the meta-connected systems, the $\downarrow\uparrow\uparrow$ state becomes the ground state, still showing

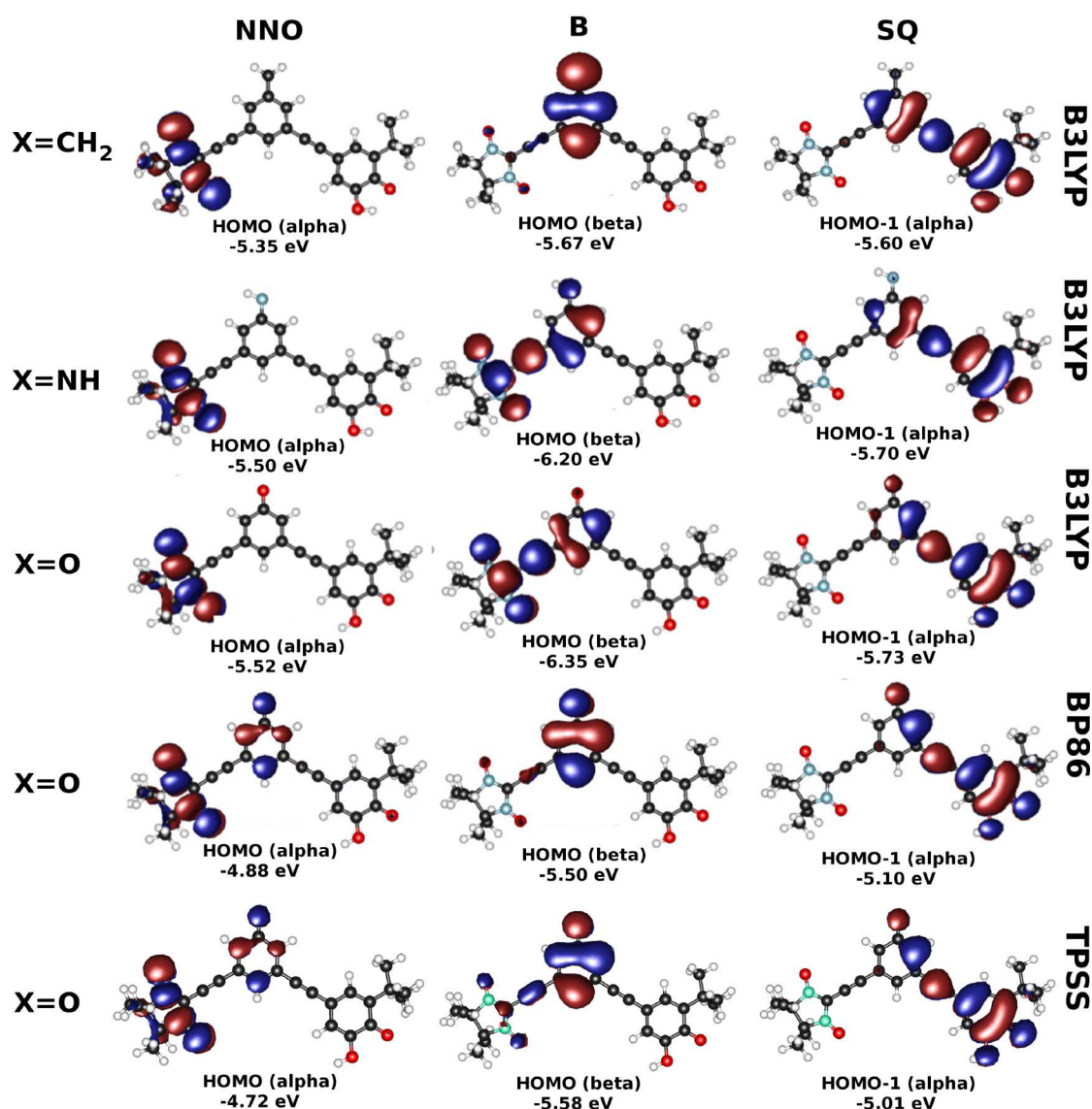


Figure 3. Top three rows: Effectively singly occupied MOs for the meta-connected triradicals for the $X=\text{CH}_2/\text{NH}/\text{O}$ radical substituents on the bridge and ethynyl spacer; $\uparrow\downarrow\uparrow$ determinant, B3LYP/def-TZVP. Bottom row: The same for $X=\text{O}$ using BP86/def-TZVP and TPSS/def-TZVP. The abbreviations at the top indicate whether the orbital is mainly located on the NNO unit, the bridge (B), or the SQ. The MOs of the $\uparrow\downarrow\uparrow$ determinant were chosen because they roughly correspond to (localized) magnetic orbitals and thus can help in qualitatively understanding exchange coupling in these systems.

antiparallel alignment between NNO and SQ, while the spin of the X radical substituent spin is oriented parallel to the spin of the SQ subunit. This is true for all three radical substituents and for all functionals. The only exception is again the B2PLYP functional, which qualitatively deviates from all other functionals in all cases. These deviations are found to be caused by the MP2 correction, which can be seen from the B2PLYP* results (without MP2 correction). Therefore, these results are not further considered in the discussion about the increase in the stabilization of the ground spin state with respect to other low-lying spin states. The B2PLYP* functional features an exact exchange admixture of 53%, which corresponds to a considerable increase compared to the other functionals employed in our study. The resulting spin state energies have the same order as that with the other functionals employed, but the energy differences are increased considerably. This further confirms the trend observed in our data: the more exact exchange, the larger the spin state energy differences.

The preference for ferromagnetic coupling between X and SQ can be rationalized by the magnetic MOs⁷⁰ located on these parts of the structure. The contours of these MOs can be used to estimate the exchange integral, which contributes to ferromagnetic coupling.⁷¹ Magnetic MOs roughly correspond to the singly occupied MOs in the BS determinant modeling the antiferromagnetically coupled state. Note that well-defined magnetic MOs could be obtained from the canonical ones by corresponding orbital transformation.⁷⁰ However, as all non-canonical MOs, the Lagrangian multipliers associated with these MOs cannot be interpreted as orbital energies. The coupling between X and SQ can therefore approximately be attributed to the HOMO^β and $\text{HOMO}-1^\alpha$ in the first three rows of Figure 3 having coefficients on shared atoms, which should lead to a nonzero exchange integral.⁷¹ The antiferromagnetic coupling between NNO and X is not obvious from similar MO arguments as both HOMO^α (located on NNO) and HOMO^β (located mainly on the bridge) for $X=$

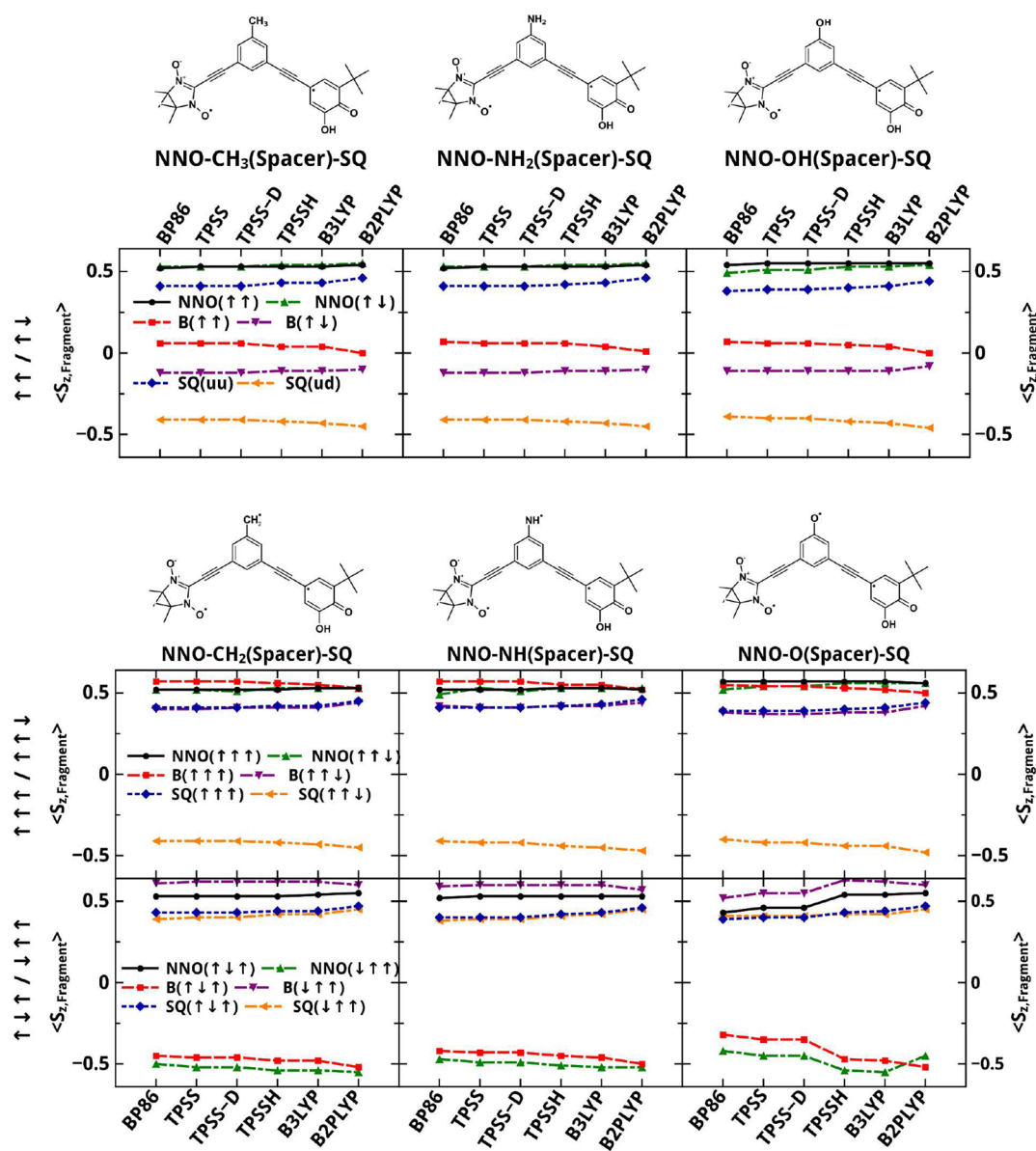


Figure 4. Mulliken local spins for the NNO, SQ, and bridge fragments calculated with different exchange–correlation functionals. Basis set: def-TZVP.

NH^\bullet and $\text{X}=\text{O}^\bullet$ share common atoms. For $\text{X}=\text{CH}_2^\bullet$, the two MOs are spatially separate, suggesting small spin coupling. This tendency in one of the MOs to localize may partially explain the different behavior of the $\text{NNO}-\text{X}$ coupling compared with the $\text{X}-\text{SQ}$ coupling. It may also explain why for $\text{X}=\text{CH}_2^\bullet$ and $\text{X}=\text{NH}^\bullet$ it is energetically more favorable to flip the spin on NNO rather than on SQ, leading to the $\uparrow\uparrow\uparrow$ spin state. The next-highest-energy spin state for these two substituents is the all-antiferromagnetic one, which can be obtained from the $\downarrow\uparrow\uparrow$ ground state by flipping the spin on the SQ, $\uparrow\downarrow\uparrow$, and the overall least favorable is the one where NNO and X couple ferromagnetically and X and SQ antiferromagnetically ($\uparrow\uparrow\downarrow$). Again, this is consistent between all functionals for those two substituents. The absolute values of spin state energy splittings are surprisingly independent of X for $\text{X}=\text{CH}_2^\bullet$ and $\text{X}=\text{NH}^\bullet$.

For $\text{X}=\text{O}^\bullet$, the situation is somewhat less clear. While the $\downarrow\uparrow\uparrow$ state is always the ground state as before, the energetic order of the remaining states depends on the exchange–correlation functional. This can be rationalized to some extent by the

dependence of the nature of the magnetic MOs on the exchange–correlation functional. For $\text{X}=\text{O}^\bullet$, the B3LYP HOMO^β shown in the third row of Figure 3 is delocalized on NNO, while the HOMO^β for TPSS (bottom row in Figure 3) is delocalized on the NNO group to a lesser extent, and for the BP86 functional, the HOMO^β is nearly fully localized on the bridge (second row from the bottom in Figure 3). The MOs obtained with pure functionals are similar in shape to the BP86 ones, and the ones obtained with hybrid functionals are similar to the B3LYP MOs. In contrast, for the other two substituents, the contours of the magnetic MOs are relatively independent of the functional. (For B2PLYP, HOMO^α and $\text{HOMO}^{\alpha-1}$ are exchanged with respect to their energetic order compared with the other hybrid functionals for all X(Spacer) structures.)

Comparing the ground-state spin configurations of the diradicals and the triradicals, the coupling between the NNO and SQ units is not changed qualitatively by the presence of the radical substituent on the bridge. However, the energy

differences between the ground state ($\downarrow\uparrow$ or $\uparrow\downarrow\uparrow$) and the next-highest state (the all-ferromagnetically coupled $\uparrow\uparrow$ or $\uparrow\uparrow\uparrow$) increase significantly in most cases. For example, considering the $\text{NNO}-\text{CH}_3(\text{Spacer})-\text{SQ}$ and $\text{NNO}-\text{CH}_2^*(\text{Spacer})-\text{SQ}$, the splitting between the all-ferromagnetically coupled state and the ground state is 4.4 (TPSS, TPSS-D, and TPSSH) to 6.2 (BP86) times larger for the radical bridge compared with that of the closed-shell bridge. For $\text{NNO}-\text{NH}_2(\text{Spacer})-\text{SQ}$ and $\text{NNO}-\text{NH}^*(\text{Spacer})-\text{SQ}$, the increase in stabilization of the $\downarrow\uparrow$ or $\uparrow\downarrow\uparrow$ state due to introduction of a radical bridge is by a factor of 4.9 (BP86) to 5.2 (B3LYP) (more details are given in Table S7 of the Supporting Information).

Interestingly, the more hybrid the character in the functional, the larger the spin state splittings (the functionals in Figure 2 are ordered from left to right according to increasing hybrid character). This is in contrast to reports of larger exact-exchange admixtures favoring the high-spin state in mononuclear transition-metal complexes.^{26,27} Exceptions to this “rule” are the $\uparrow\downarrow\uparrow$ states and all BP86 spin state energies for the O(Spacer) bridge when compared with TPSS. The reason for this unconventional behavior may be that the NNO and SQ radical units feature qualitatively very different spin density distributions, which results in bridges that usually couple ferromagnetically (such as meta-connected benzene units), now leading to antiferromagnetic coupling and vice versa for *para*-phenylene bridges.^{4,72} Note that in this work, different functionals are employed primarily to ensure that our qualitative conclusions are not an artifact of an arbitrarily chosen functional. The behavior found for the systems under study here differing from transition-metal complexes is highly interesting but will be left for future work due to the reasons just mentioned.

Adding an empirical dispersion correction minimally influences spin state energetics, as can be seen by comparing the TPSS and TPSS-D results, except for a slight downshift of energies relative to the $\uparrow\uparrow\uparrow$ state for the O(Spacer) bridge upon adding the correction term. Additional MO plots for all spin states are provided in section 5 of the Supporting Information.⁴⁰

4.1.2. Local Spins. Local spins summed over the relevant parts of the structures under study (NNO radical unit, bridge B, SQ radical unit) are a valuable tool for quantifying changes in molecular electronic structure. In Figure 4, these sums over local spins calculated from the Mulliken partitioning scheme (see eq 1) are reported for all structures, spin states, and functionals under study. A (summed-up) local spin of 0.5 au corresponds to one unpaired electron located on a specific fragment of the molecular structure. The bridges have been defined to include the $\text{C}\equiv\text{C}$ spacers. Selected plots of the spin densities may be found in the Supporting Information.⁴⁰

A part of the SQ's spin is delocalized on the bridge. This portion decreases from about 0.07 to 0 with increasing exact exchange in the functional for all systems under study. This corresponds to the well-known trend of more pronounced spin localization for a larger exact exchange admixture (compare, e.g., ref 38). Also, for all other systems, there is a clear trend toward more spin localization on the NNO and SQ radical units with an increasing exact exchange admixture, while the spin on the bridge increases or decreases depending on the relative spin orientation compared to the NNO and SQ units. In most cases, the variation of the subsystems' local spins does not exceed 0.07. The main exceptions are the two $\text{X}=\text{O}$ systems, for which the most pronounced variations with respect

to the functional had already been found in the spin state energetics and the nature of the MOs.

4.2. Comparison with Second-Generation Computational Models: Toward Possible Synthetic Targets. The model systems discussed above feature chemically unstable spin centers on the bridge. Another concern is the SQ unit, which needs to be stabilized, for example, by a coordinated zinc complex ion as in the experimentally studied systems.⁴ Also, introducing ethynyl spacers may prove to be a synthetic challenge. To test how far these findings for the model systems can be transferred to structures that are likely accessible by chemical synthesis, we compare our results with the triradical $\text{NNO}-\text{NO}-\text{SQ}(\text{Zn})$, where “NO” is a stable nitroxyl-based radical substituent (Figure 2) and its analogous closed-shell bridge diradical $\text{NNO}-\text{NOH}-\text{SQ}(\text{Zn})$ is obtained by adding a hydrogen. We “interpolate” between the simple model systems and the possible synthetic target by changing in a stepwise fashion the three features that distinguish them. Thus, we compare the following four structures: $\text{NNO}-\text{NH}(\text{spacer})-\text{SQ}$, $\text{NNO}-\text{NH}-\text{SQ}$, $\text{NNO}-\text{NH}-\text{SQ}(\text{Zn})$, and $\text{NNO}-\text{NO}-\text{SQ}(\text{Zn})$. The B2PLYP functional has not been considered here because it always displayed qualitative deviations from the other functionals in the previous section.

The nature of the ground state does not change when going from a simple model system to a possible synthetic target; for all four structures under discussion in this section, the energetically most stable spin orientation is $\downarrow\uparrow$ for the diradicals and $\downarrow\uparrow\uparrow$ for the spin-polarized bridge triradicals (see Figure 2 bottom row; for coupling constants, see the Supporting Information). The magnetic exchange coupling constants for the potentially synthesizable system are found to be between -14.2 (BP86) and -38.5 cm^{-1} (B3LYP). This is the same order of magnitude as the coupling constant experimentally determined for an analogous *meta*-phenylene bridged diradical (without NOH substituent) as synthesized by one of the authors,⁷² which was found to be -31.8 cm^{-1} . As above, spin state energy splittings generally increase with the increasing exact exchange admixture in the exchange–correlation functional. The energetic ordering of the different spin states is also quite unaffected by the details of the structure and the functional, except for a crossover between the $\uparrow\downarrow\uparrow$ and $\uparrow\uparrow\uparrow$ orientations at higher exact exchange for the Zn-containing structures.

For the closed-shell bridge diradicals, introducing ethynyl spacers decreases spin state energy splittings, as expected. Binding the Zn(II) ion to the SQ radical has the same effect, which appears to be related to the larger torsional angle between the $\text{SQ}(\text{Zn})$ moiety and the bridge originating from the sterically demanding zinc complex (Table S8 in the Supporting Information). This possibly leads to weaker communication when compared with the $\text{NNO}-\text{NH}-\text{SQ}$ complex. For the triradicals, this decrease is surprisingly less pronounced. However, replacing the model radical substituent NH by the more synthetically accessible sterically protected nitroxyl radical leads to significantly reduced absolute spin state energy splittings for the triradicals.

From a qualitative point of view, in the $\text{NNO}-\text{NO}-\text{SQ}(\text{Zn})$ system, the stabilization of the ground state with respect to the next-highest spin state ranges from 3.0 for TPSS-D and B3LYP to 3.5 for TPSS, while they are about twice as large in the $\text{NNO}-\text{NH}-\text{SQ}(\text{Zn})$ model system, where the stabilization is between 5.5 for TPSS-D and 6.0 for TPSSH and B3LYP. This is found to correlate with the much lower degree of spin

delocalization on the phenyl ring for the NO-substituted bridge. For the NH system, 40–47% of the total spin is found on the phenyl ring (depending on the spin state and the functional), while in the case of the NO triradical, the spin contributions on the phenyl ring are between 6 and 24% (see also Table S6 in the Supporting Information). The effect of this substitution is less pronounced for the diradicals. Still, the overall conclusions that can be drawn from the model systems are highly transferable to a system that may be synthetically achievable.

5. CONCLUSIONS

In this work, we have studied the stabilization of the ground state with respect to spin flips that derive from introducing a spin on the bridge for a range of meta- (and para-connected) benzene-ring-based bridges connecting a NNO and a SQ radical unit. Replacing a closed-shell substituent on the bridge by a radical substituent $X=CH_2^\bullet$ or $X=NH^\bullet$ increases this stabilization by a factor of about 3–6. However, it should be noted that for all systems the B2PLYP functional qualitatively deviates from all other functionals. This suggests that radical bridges are an effective means of stabilizing the ground-state spin configurations. Systems possessing an $X=O^\bullet$ substituent are much more sensitive to the choice of exchange–correlation functional than both their closed-shell analogues and the equivalent triradicals with $X=CH_2^\bullet$ or $X=NH^\bullet$. The $X=O$ model systems may serve as a starting point for simplified small-model systems that can be treated by accurate correlated electronic structure methods. If they show the same erratic dependence on the functional as the $X=O$ systems that we have studied here, they may serve as sensitive test cases for evaluating and constructing more reliable exchange–correlation functionals for spin state energetics.

Comparing our model systems with a potentially synthesizable meta-bridged structure revealed good qualitative agreement in terms of spin state energetics. The potentially realizable complex discussed in this work shows a maximal stabilization of the ground state up to a factor of 3.5 compared with that of the diradical, while for the model systems and complexes constructed as interpolations between the two, the stabilization may be up to twice as large (e.g., a factor of 6). Furthermore, the absolute spin state energy splittings are smaller in the potentially stable complex. This difference is mainly attributed to the change of the radical substituent from a simple NH group in the simple model to a sterically protected nitroxyl group in the possible synthetic target. This is in line with the decreasing delocalization of spin density from the radical substituent onto the phenyl ring, underlining the crucial influence of the bridge. To obtain an optimal stabilization of the ground state with respect to spin flips, further effort must be expended in the study of different radical bridges and how they affect spin state energetics. These considerations will be addressed in future work.

■ ASSOCIATED CONTENT

● Supporting Information

The Supporting Information is available free of charge on the ACS Publications website at DOI: 10.1021/acs.jpca.6b07270.

Additional molecular orbital plots, local spins for the systems in section 4.2, spin densities, Heisenberg coupling constants, structural parameters, molecular Cartesian coordinates, and results for para-substituted model systems (PDF)

■ AUTHOR INFORMATION

Corresponding Author

*E-mail: carmen.herrmann@chemie.uni-hamburg.de. Phone: +49 (0)40 42838 6934.

ORCID

Carmen Herrmann: 0000-0002-9496-0664

Notes

The authors declare no competing financial interest.

■ ACKNOWLEDGMENTS

C.H. and T.S. acknowledge financial support from the DFG via SFB 668, from the Free and Hanseatic City of Hamburg in the context of the Landesexzellenzinitiative Hamburg “Nanospintronics”, and from the Fonds der Chemischen Industrie. D.A.S. thanks the National Science Foundation (CHE-1464085 and CHE-1213269) for financial support. M.L.K. acknowledges the National Science Foundation (NSF CHE 1565930 and NSF #IIA-1301346) for financial assistance. C.H. and T.S. would further like to thank the University of Hamburg High Performance Computing Centre for computational resources and Markus Reiher at ETH Zurich for access to our implementations in a local version of TURBOMOLE.

■ REFERENCES

- (1) Kahn, O. *Molecular Magnetism*; Wiley VCH: New York, 1993.
- (2) Sanvito, S. Molecular Spintronics. *Chem. Soc. Rev.* **2011**, *40*, 3336–3355.
- (3) Terencio, T.; Bastardis, R.; Suaud, N.; Maynau, D.; Bonvoisin, J.; Malrieu, J. P.; Calzado, C. J.; Guihery, N. Physical Analysis of the Through-Ligand Long-Distance Magnetic Coupling: Spin-Polarization Versus Anderson Mechanism. *Phys. Chem. Chem. Phys.* **2011**, *13*, 12314–12320.
- (4) Kirk, M. L.; Shultz, D. A.; Stasiw, D. E.; Lewis, G. F.; Wang, G.; Brannen, C. L.; Sommer, R. D.; Boyle, P. D. Superexchange Contributions to Distance Dependence of Electron Transfer/Transport: Exchange and Electronic Coupling in Oligo(para-Phenylene)- and Oligo(2,5-Thiophene)-Bridged Donor-Bridge-Acceptor Biradical Complexes. *J. Am. Chem. Soc.* **2013**, *135*, 17144–17154.
- (5) Hoffmann, S. K.; Hilczler, W.; Goslar, J. Weak Long-Distance Superexchange Interaction and Its Temperature Variations in Copper(II) Compounds Studied by Single Crystal EPR. *Appl. Magn. Reson.* **1994**, *7*, 289–321.
- (6) Coffman, R. E.; Buettner, G. R. A Limit Function for Long-Range Ferromagnetic and Antiferromagnetic Superexchange. *J. Phys. Chem.* **1979**, *83*, 2387–2392.
- (7) Rinehart, J. D.; Fang, M.; Evans, W. J.; Long, J. R. Strong Exchange and Magnetic Blocking in N_2^{3-} Radical-Bridged Lanthanide Complexes. *Nat. Chem.* **2011**, *3*, 538–542.
- (8) Rinehart, J. D.; Long, J. R. Exploiting Single-Ion Anisotropy in the Design of f-Element Single-Molecule Magnets. *Chem. Sci.* **2011**, *2*, 2078.
- (9) Rinehart, J. D.; Fang, M.; Evans, W. J.; Long, J. R. A N_2^{3-} Radical-Bridged Terbium Complex Exhibiting Magnetic Hysteresis at 14 K. *J. Am. Chem. Soc.* **2011**, *133*, 14236–14239.
- (10) Demir, S.; Jeon, I.-R.; Long, J. R.; Harris, T. D. Radical Ligand-Containing Single-Molecule Magnets. *Coord. Chem. Rev.* **2015**, *289–290*, 149–176. Progress in Magnetochemistry.
- (11) Demir, S.; Zadrozny, J. M.; Nippe, M.; Long, J. R. Exchange Coupling and Magnetic Blocking in Bipyrimidyl Radical-Bridged Dilanthanide Complexes. *J. Am. Chem. Soc.* **2012**, *134*, 18546–18549.
- (12) Mei, X.; Wang, X.; Wang, J.; Ma, Y.; Li, L.; Liao, D. Dinuclear Lanthanide Complexes Bridged by Nitronyl Nitroxide Radical Ligands with 2-Phenolate Groups: Structure and Magnetic Properties. *New J. Chem.* **2013**, *37*, 3620–3626.
- (13) Liu, R.; Zhang, C.; Li, L.; Liao, D.; Sutter, J.-P. Ligand Substitution Effect on Single-Molecule Magnet Behavior in Dinuclear

Dysprosium Complexes with Radical Functionalized Phenol as Bridging Ligands. *Dalton Trans.* **2012**, *41*, 12139–12144.

(14) Jeon, I.-R.; Park, J. G.; Xiao, D. J.; Harris, T. D. An Azophenine Radical-Bridged Fe₂ Single-Molecule Magnet With Record Magnetic Exchange Coupling. *J. Am. Chem. Soc.* **2013**, *135*, 16845–16848.

(15) Dechambenoit, P.; Long, J. R. Microporous Magnets. *Chem. Soc. Rev.* **2011**, *40*, 3249.

(16) Wu, Y.-n.; Zhou, M.; Li, S.; Li, Z.; Li, J.; Wu, B.; Li, G.; Li, F.; Guan, X. Magnetic Metal-Organic Frameworks: γ -Fe₂O₃@MOFs via Confined In Situ Pyrolysis Method for Drug Delivery. *Small* **2014**, *10*, 2927–2936.

(17) Tranchemontagne, D. J.; Mendoza-Cortes, J. L.; O’Keeffe, M.; Yaghi, O. M. Secondary Building Units, Nets and Bonding in the Chemistry of Metal-Organic Frameworks. *Chem. Soc. Rev.* **2009**, *38*, 1257–1283.

(18) Kaskel, S., Ed. *The Chemistry of Metal-Organic Frameworks: Synthesis, Characterization, and Applications*; Wiley VCH: New York, 2016.

(19) Faust, T. B.; D’Alessandro, D. M. Radicals in Metal-Organic Frameworks. *RSC Adv.* **2014**, *4*, 17498.

(20) Xu, F.; Xu, H.; Chen, X.; Wu, D.; Wu, Y.; Liu, H.; Gu, C.; Fu, R.; Jiang, D. Radical Covalent Organic Frameworks: A General Strategy to Immobilize Open-Accessible Polyradicals for High-Performance Capacitive Energy Storage. *Angew. Chem., Int. Ed.* **2015**, *54*, 6814–6818.

(21) McKinnon, S. D. J.; Patrick, B. O.; Lever, A. B. P.; Hicks, R. G. Binuclear Ruthenium Complexes of a Neutral Radical Bridging Ligand. A New “Spin” on Mixed Valency. *Inorg. Chem.* **2013**, *52*, 8053–8066.

(22) Sarkar, B.; Patra, S.; Fiedler, J.; Sunoj, R. B.; Janardanan, D.; Lahiri, G. K.; Kaim, W. Mixed-Valent Metals Bridged by a Radical Ligand: Fact Or Fiction Based on Structure-Oxidation State Correlations. *J. Am. Chem. Soc.* **2008**, *130*, 3532–3542.

(23) Chernick, E. T.; Mi, Q.; Kelley, R. F.; Weiss, E. A.; Jones, B. A.; Marks, T. J.; Ratner, M. A.; Wasielewski, M. R. Electron Donor-Bridge-Acceptor Molecules with Bridging Nitronyl Nitroxide Radicals: Influence of a Third Spin on Charge- and Spin-Transfer Dynamics. *J. Am. Chem. Soc.* **2006**, *128*, 4356–4364.

(24) Chernick, E. T.; Mi, Q.; Vega, A. M.; Lockard, J. V.; Ratner, M. A.; Wasielewski, M. R. Controlling Electron Transfer Dynamics in Donor-Bridge-Acceptor Molecules by Increasing Unpaired Spin Density on the Bridge. *J. Phys. Chem. B* **2007**, *111*, 6728–6737.

(25) Kirk, M. L.; Shultz, D. A.; Schmidt, R. D.; Habel-Rodriguez, D.; Lee, H.; Lee, J. Ferromagnetic Nanoscale Electron Correlation Promoted by Organic Spin-Dependent Delocalization. *J. Am. Chem. Soc.* **2009**, *131*, 18304–18313.

(26) Reiher, M.; Salomon, O.; Hess, B. A. Reparameterization of Hybrid Functionals Based on Energy Differences of States of Different Multiplicity. *Theor. Chem. Acc.* **2001**, *107*, 48–55.

(27) Harvey, J. N. DFT Computation of Relative Spin-State Energetics of Transition Metal Compounds. *Struct. Bonding* **2004**, *112*, 151–184.

(28) Grimme, S. Semiempirical Hybrid Density Functional with Perturbative Second-Order Correlation. *J. Chem. Phys.* **2006**, *124*, 034108.

(29) Grimme, S. Density Functional Theory with London Dispersion Corrections. *Wiley Interdisciplinary Reviews: Computational Molecular Science* **2011**, *1*, 211–228.

(30) Herrmann, C.; Solomon, G. C.; Ratner, M. A. Organic Radicals as Spin Filters. *J. Am. Chem. Soc.* **2010**, *132*, 3682–3684.

(31) Anderson, P. W. New Approach to the Theory of Superexchange Interactions. *Phys. Rev.* **1959**, *115*, 2–13.

(32) Bertrand, P. Electron Transfer between Biological Molecules Coupled by an Exchange Interaction. *Chem. Phys. Lett.* **1985**, *113*, 104–107.

(33) Brunold, T. C.; Gamelin, D. R.; Solomon, E. I. Excited-State Exchange Coupling in Bent Mn(III) – O – Mn(III) Complexes: Dominance of the π/σ Superexchange Pathway and Its Possible Contributions to the Reactivities of Binuclear Metalloproteins. *J. Am. Chem. Soc.* **2000**, *122*, 8511–8523.

(34) Herrmann, C.; Elmsiz, J. Electronic Communication Through Molecular Bridges. *Chem. Commun.* **2013**, *49*, 10456–10458.

(35) Proppe, J.; Herrmann, C. Communication Through Molecular Bridges: Different Bridge Orbital Trends Result in Common Property Trends. *J. Comput. Chem.* **2015**, *36*, 201–209.

(36) Noodleman, L. Valence Bond Description Of Antiferromagnetic Coupling in Transition Metal Dimers. *J. Chem. Phys.* **1981**, *74*, 5737–5743.

(37) Clark, A. E.; Davidson, E. R. Local Spin. *J. Chem. Phys.* **2001**, *115*, 7382–7392.

(38) Herrmann, C.; Reiher, M.; Hess, B. A. Comparative Analysis of Local Spin Definitions. *J. Chem. Phys.* **2005**, *122*, 034102.

(39) Mayer, I. Local Spins: An Alternative Treatment For Single Determinant Wave Functions. *Chem. Phys. Lett.* **2007**, *440*, 357–359.

(40) See the [Supporting Information](#).

(41) Parr, R. G.; Yang, W. In *Density-Functional Theory of Atoms and Molecules*; Breslow, R., Goodenough, J. B., Halpern, J., Rowlinson, J. S., Eds.; International Series of Monographs on Chemistry; Oxford Science Publications: New York, 1989; Vol. 16.

(42) von Barth, U.; Hedin, L. A Local Exchange-Correlation Potential for the Spin Polarized Case: I. *J. Phys. C: Solid State Phys.* **1972**, *5*, 1629–1642.

(43) Perdew, J.; Savin, A.; Burke, K. Escaping the Symmetry Dilemma Through a Pair-Density Interpretation of Spin-Density Functional Theory. *Phys. Rev. A: At., Mol., Opt. Phys.* **1995**, *51*, 4531–4541.

(44) Perdew, J. P.; Ernzerhof, M.; Burke, K.; Savin, A. On-Top Pair-Density Interpretation of Spin Density Functional Theory, with Applications To Magnetism. *Int. J. Quantum Chem.* **1997**, *61*, 197–205.

(45) Jacob, C.; Reiher, M. Spin in Density-Functional Theory. *Int. J. Quantum Chem.* **2012**, *112*, 3661–3684.

(46) Pople, J. A.; Gill, P. M. W.; Handy, N. C. Spin-Unrestricted Character of Kohn-Sham Orbitals for Open-Shell Systems. *Int. J. Quantum Chem.* **1995**, *56*, 303–305.

(47) Wang, J.; Becke, A. D.; Smith, V. H., Jr. Evaluation of $\langle \hat{S}^2 \rangle$ in Restricted, Unrestricted Hartree-Fock, and Density Functional Based Theories. *J. Chem. Phys.* **1995**, *102*, 3477–3480.

(48) Cohen, A. J.; Tozer, D. J.; Handy, N. C. Evaluation of $\langle \hat{S}^2 \rangle$ in Density Functional Theory. *J. Chem. Phys.* **2007**, *126*, 214104.

(49) Görling, A.; Levy, M.; Perdew, J. P. Expectation Values in Density-Functional Theory, and Kinetic Contribution to the Exchange-Correlation Energy. *Phys. Rev. B: Condens. Matter Mater. Phys.* **1993**, *47*, 1167–1173.

(50) Bauer, G. E. W. General Operator Ground-State Expectation Values in the Hohenberg-Kohn-Sham Density-Functional Formalism. *Phys. Rev. B: Condens. Matter Mater. Phys.* **1983**, *27*, 5912–5918.

(51) Li Manni, G.; Carlson, R. K.; Luo, S.; Ma, D.; Olsen, J.; Truhlar, D. G.; Gagliardi, L. Multiconfiguration Pair-Density Functional Theory. *J. Chem. Theory Comput.* **2014**, *10*, 3669–3680.

(52) Hubert, M.; Hedegard, E. D.; Jensen, H. J. A. Investigation of Multiconfigurational Short-Range Density Functional Theory for Electronic Excitations in Organic Molecules. *J. Chem. Theory Comput.* **2016**, *12*, 2203–2213.

(53) Clark, A. E.; Davidson, E. R. Population Analyses That Utilize Projection Operators. *Int. J. Quantum Chem.* **2003**, *93*, 384–394.

(54) Mulliken, R. S. Electronic Population Analysis on LCAO-MO Molecular Wave Functions I. *J. Chem. Phys.* **1955**, *23*, 1833–1840.

(55) Szabo, A.; Ostlund, N. S. *Modern Quantum Chemistry: Introduction to Advanced Electronic Structure Theory*; Dover Publications: New York, 1996.

(56) Becke, A. D. Density-Functional Exchange-Energy Approximation with Correct Asymptotic Behavior. *Phys. Rev. A: At., Mol., Opt. Phys.* **1988**, *38*, 3098–3100.

(57) Perdew, J. P. Density-Functional Approximation for the correlation energy of the inhomogeneous electron gas. *Phys. Rev. B: Condens. Matter Mater. Phys.* **1986**, *33*, 8822–8824.

(58) Tao, J.; Perdew, J. P.; Staroverov, V. N.; Scuseria, G. E. Climbing the Density Functional Ladder: Nonempirical Meta-Generalized

Gradient Approximation Designed for Molecules and Solids. *Phys. Rev. Lett.* **2003**, *91*, 146401–146404.

(59) Perdew, J. P.; Tao, J.; Staroverov, V. N.; Scuseria, G. E. Meta-Generalized Gradient Approximation: Explanation of a Realistic Nonempirical Density Functional. *J. Chem. Phys.* **2004**, *120*, 6898–6911.

(60) Becke, A. D. Density-Functional Thermochemistry. III. The Role of Exact Exchange. *J. Chem. Phys.* **1993**, *98*, 5648–5652.

(61) Lee, C.; Yang, W.; Parr, R. G. Development of the Colle-Salvetti Correlation-Energy Formula into a Functional of the Electron Density. *Phys. Rev. B: Condens. Matter Mater. Phys.* **1988**, *37*, 785–789.

(62) Schäfer, A.; Huber, C.; Ahlrichs, R. Fully Optimized Contracted Gaussian Basis Sets of TripleZeta Valence Quality for Atoms Li to Kr. *J. Chem. Phys.* **1994**, *100*, 5829–5835.

(63) http://www.ftpstatus.com/dir_properties.php?sname=ftp.chemie.uni-karlsruhe.de&did=22 (Nov 26, 2016).

(64) http://www.ftpstatus.com/dir_properties.php?sname=ftp.chemie.uni-karlsruhe.de&did=33 (Nov 26, 2016).

(65) Ahlrichs, R.; Bär, M.; Häser, M.; Horn, H.; Kölmel, C. Electronic Structure Calculation on Workstation Computers: The Program System Turbomole. *Chem. Phys. Lett.* **1989**, *162*, 165–169.

(66) TURBOMOLE, a development of University of Karlsruhe and Forschungszentrum Karlsruhe GmbH, 1989–2007, TURBOMOLE GmbH, since 2007. <http://www.turbomole.com> (Nov 26, 2016).

(67) Herrmann, C.; Podewitz, M.; Reiher, M. Restrained Optimization of Broken-Symmetry Determinants. *Int. J. Quantum Chem.* **2009**, *109*, 2430–2446.

(68) (a) Schaftenaar, G.; Noordik, J. Molden: A Pre- and Post-Processing Program for Molecular and Electronic Structures. *J. Comput.-Aided Mol. Des.* **2000**, *14*, 123–134. (b) MOLDEN. <http://www.cmbi.ru.nl/molden/molden.html> (Nov 26, 2016).

(69) POV-Ray. <http://www.povray.org/> (Nov 26, 2016).

(70) Neese, F. Definition of Corresponding Orbitals and the Diradical Character in Broken Symmetry DFT Calculations on Spin Coupled Systems. *J. Phys. Chem. Solids* **2004**, *65*, 781–785.

(71) Hay, P. J.; Thibeault, J. C.; Hoffmann, R. Orbital Interactions in Metal Dimer Complexes. *J. Am. Chem. Soc.* **1975**, *97*, 4884–4899.

(72) Kirk, M. L.; Shultz, D. A.; Stasiw, D. E.; Habel-Rodriguez, D.; Stein, B.; Boyle, P. D. Electronic And Exchange Coupling in a Cross-Conjugated D-B-A Biradical: Mechanistic Implications for Quantum Interference Effects. *J. Am. Chem. Soc.* **2013**, *135*, 14713–14725.